Bull. Mater. Sci., Vol. 40, No. 3, June 2017, pp. 505–511
DOI 10.1007/s12034-017-1385-1

Ultrasonic-assisted fabrication of superhydrophobic ZnO nanowall films

S SUTHA[1], R T RAJENDRA KUMAR[2], BALDEV RAJ[3] and K R RAVI[1,*]
[1]PSG Institute of Advanced Studies, Coimbatore 641 004, India
[2]Department of Nanoscience and Technology, Bharathiar University, Coimbatore 641 046, India
[3]National Institute of Advance Studies, Bangalore 560 012, India
*Author for correspondence (krravi.psgias@gmail.com)

MS received 25 May 2016; accepted 22 July 2016; published online 9 June 2017

Abstract. Zinc oxide-based superhydrophobic surfaces were fabricated on aluminium oxide-seeded glass substrates via sonochemical approach by varying the parameter, the sonication time duration. The fabricated structures have nanowall-like morphology with an average long axis length and thickness of ∼300 and ∼40 nm, respectively. The surface roughness created by surface-modified ZnO nanowalls and the air pockets trapped within the dense nanowalls, transformed the hydrophobic glass substrates into superhydrophobic surfaces with water contact angle of 156° during 20 min of sonication. An independent analysis was carried out to study the growth of ZnO nanowalls over glass substrates in the absence of the aluminium oxide seed layer and sonication process. The results suggested that the synergistic effect of the aluminium oxide seed layer and sonochemical process can enable the formation of ZnO nanowall structures favourable for superhydrophobic property. A possible growth mechanism of ZnO nanowalls formation during sonication process has been discussed in detail.

Keywords. Zinc oxide nanowalls; sonication; superhydrophobicity.

1. Introduction

Superhydrophobic surfaces are biologically inspired from the lotus leaf as its classical example. Nano-level surface roughness along with low surface energy enables water droplets to remain spherical with a static water contact angle greater than 150° on such surfaces. In the recent past, many attempts have been made to fabricate superhydrophobic coatings on glass substrates using various methods, namely: chemical vapour deposition, dip, spin and spray coating, electro-spinning, sputtering, nano-imprint lithography and electron beam evaporation [1]. Sonochemical technique has been recently emerging as a rapid, cost-effective technique to deposit nanostructures over diverse substrates [2–5]. Jung *et al* [2] demonstrated the sonication-assisted *in-situ* growth of ZnO nanorods with an average growth rate of 500 nm h^{-1} on Zn-seeded glass substrates. Perelshtein *et al* [3] sonochemically deposited ZnO nanoparticles with average particle size of approximately 300 nm on cotton bandages for antibacterial applications. Oh *et al* [4] utilized the sonochemical technique for vertical growth of ZnO nanorods on patterned substrates for resistive-type gas sensor applications. Nayak *et al* [5] reported the growth of ZnO nanorods from ZnO seed layer using the sonochemical technique for low-cost electronics, photonics and energy conversion applications. Okyay *et al* [6] grew ZnO nanorods on ZnO seeded glass substrates purely based on sonochemical technique for antimicrobial applications.

As per the literature review, there are no reports regarding the growth of ZnO nanowalls on glass substrates using the sonochemical technique for creating superhydrophobic surfaces. Hence, in the present work, an attempt has been made to fabricate *in-situ* grown ZnO nanowalls over seeded glass substrates via sonochemical technique to achieve superhydrophobic property.

2. Materials and methods

In the present work, ZnO nanowall based superhydrophobic glass surfaces were fabricated. For this purpose, microscopic glass slides were taken as substrate. The synthesis procedure involved the following three steps, (1) *Aluminium oxide seed layer formation:* initially, $Al(NO_3)_3 \cdot 9H_2O$ (1 M) was dissolved in 2-methoxyethanol (10 ml) in the presence of monoethanolamine as a stabilizer. The resultant mixture was left for hydrolysis under magnetic stirring for 2 h and utilized as sol for spin coating. The sol was spin-coated on glass substrates at 3000 RPM for 60 s and annealed at 400°C for 60 min to form aluminium oxide seed layers. (2) *Formation of ZnO nanostructures:* seeded substrate was placed horizontally at the bottom of the beaker containing equimolar (0.02 M) concentration of $Zn(NO_3)_2 \cdot 6H_2O$ and $(CH_2)_6N_4$. Ultrasonic waves (Ultrasonic Processor, Sonics and Systems, 500 W, 20 kHz at 20% efficiency) were introduced in the solution for 5, 10, 15, 20, 25 and 30 min under ambient conditions.

After this process, the glass substrate was washed and dried at room temperature. (3) *Low surface energy modification of substrates:* the chemical modification was done by spin coating of 1H, 1H, 2H, 2H-perfluorooctyltrichlorosilane solution followed by annealing at 180° for 30 min. Hereafter, this fabrication process will be referred as technique 1.

To determine the role of aluminium oxide seed layer and the sonication process independently on superhydrophobic property of ZnO nanowall surfaces, two set of experiments were carried out and the results were compared. For these comparative studies, the above-mentioned procedure was repeated with minor changes: (1) the aluminium oxide-seeded substrates were placed in a beaker (containing ZnO precursor solution) under magnetic stirring without sonication for 5 to 30 min (denoted as technique 2); (2) the substrates without aluminium oxide seed layer were placed in a beaker (containing ZnO precursor solution) under sonication for 5 to 30 min (denoted as technique 3).

The crystalline nature and growth direction of the deposited nanostructures were investigated using transmission electron microscopy (TEM, JEOL JEM 2100). For TEM analysis, the nano-deposits were removed from the glass substrate by subjecting it into the bath sonication in ethanol medium for 10 min. The surface morphology of the fabricated substrates was analysed using field emission gun scanning electron microscopy (FESEM, Carl Zeiss, Carl Zeiss Microscopy Ltd) and atomic force microscopy (AFM, NTMDT, Russia). The superhydrophobic nature of the fabricated substrates was analysed using a contact angle meter (KRÜSS, DSA 20E) armed with a CCD camera module.

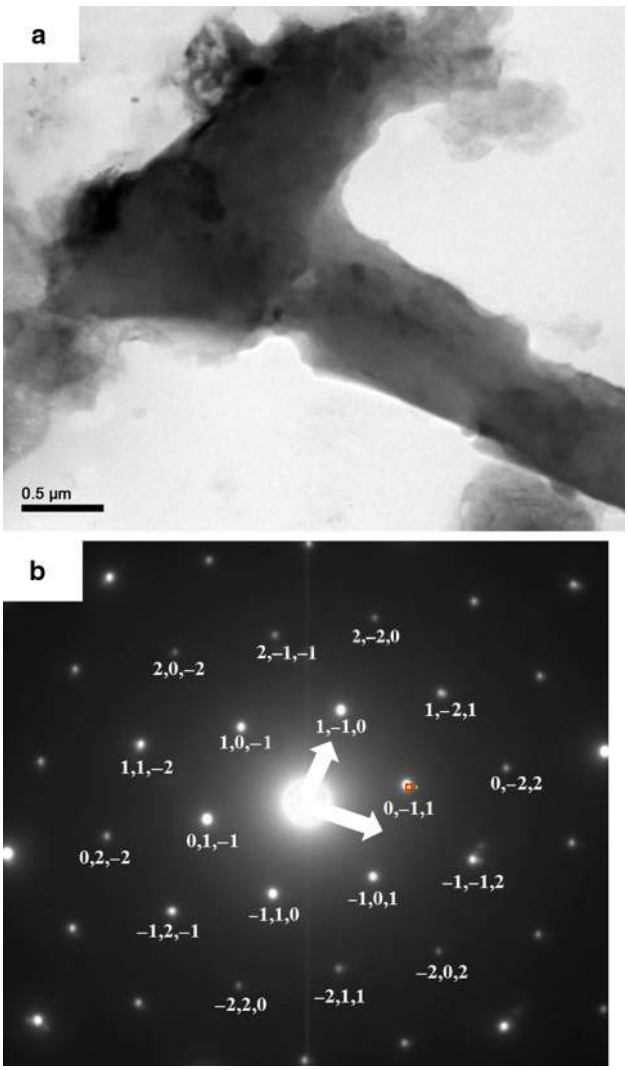

Figure 1. (**a**) Bright field TEM image of ZnO nanowalls (fabricated using technique 1 for 30 min) and (**b**) the corresponding SAED pattern.

3. Results and discussion

The crystal nature of the fabricated structure (30-min sonicated sample) was investigated using low-magnification TEM and selected-area electron diffraction (SAED) pattern, shown in figure 1. Figure 1a displays the morphology of delaminated nanowall networks from the glass substrate. Figure 1b shows the corresponding SAED pattern of TEM image, where regularly spaced spots can be seen; indicating that the fabricated material was ZnO and it was in highly crystalline nature. Further, SAED pattern taken under [1 1 1] zone axis demonstrated that the ZnO nanowalls were grown along [1 –1 0] and [–1 –1 2] directions.

Figure 2 explicitly shows the influence of sonication time on the morphology of ZnO nanostructures in the presence of aluminium oxide seed layer. From figure 2a, it is clear that the spin-coated aluminium oxide seed layer has the particles of size less than 100 nm in diameter. The purpose of introducing a seed layer is that they can effectively reduce the interfacial energy between the crystal nuclei and the substrate; thereby, reducing the nucleation barrier for the one- and two-dimensional growth of nanostructures [7]. According to figure 2b–g, it can be inferred that the density of nanowalls is heavily dependent on the sonication time. Till 10 min of sonication, a large number of thin nanowalls tend to grow randomly from the surface of the aluminium oxide seed layer. The crinkly ZnO nanowalls were found to be grown perpendicularly from the seeded substrate and top edges of some of them were slightly twisted, which is an intrinsic characteristic of 2D nanostructures [8]. The average long axis length of nanowalls for 5- and 10-min sonicated samples was measured as 478 ± 25 and 259 ± 14 nm, respectively and the average thickness of nanowalls were ranging from 30 to 40 nm (figure 2b and c). The decrease in the average long axis length of the nanowalls with the increase in sonication time suggested that there might be growth of nanowalls from the nucleation sites in the faces of 5-min sonicated samples. As the sonication time increased to 15 min, the average long axis length of the nanowalls further reduced to 172 ± 8 nm, suggesting that the density of nanowalls increased further by blocking the

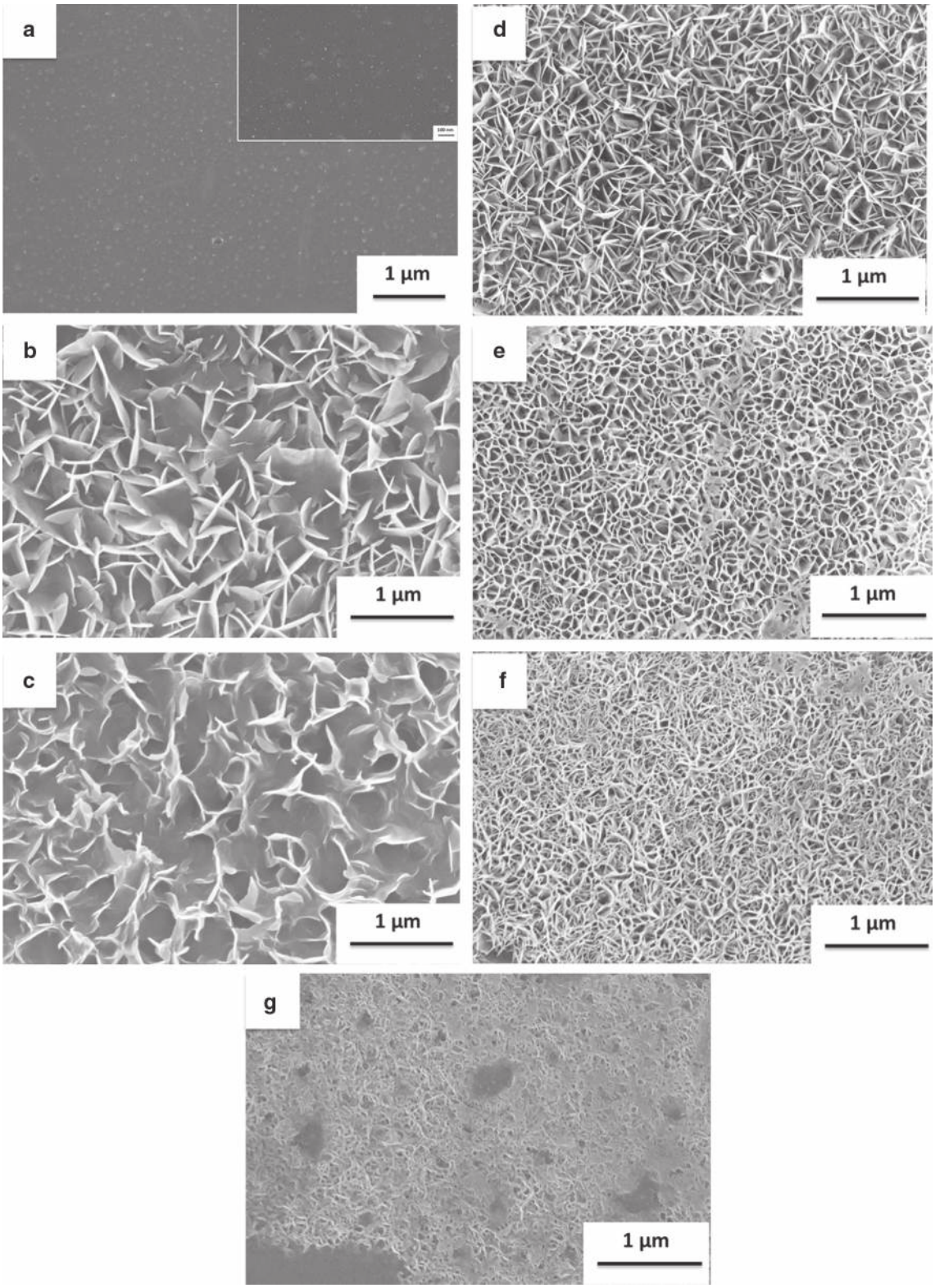

Figure 2. FESEM images of (**a**) aluminium oxide seed layer; seeded glass substrates subjected to sonication for (**b**) 5, (**c**) 10, (**d**) 15, (**e**) 20, (**f**) 25 and (**g**) 30 min.

long axis growth (figure 2d). When sonication time reached 20 min, there was a growth of superficial layer of nanowalls with long axis length of 95 nm, which could be seen over the previously formed layers (figure 2e). With further increase in sonication time, there was multilayer growth of nanowalls with two to five nanowalls combined together to form a dense

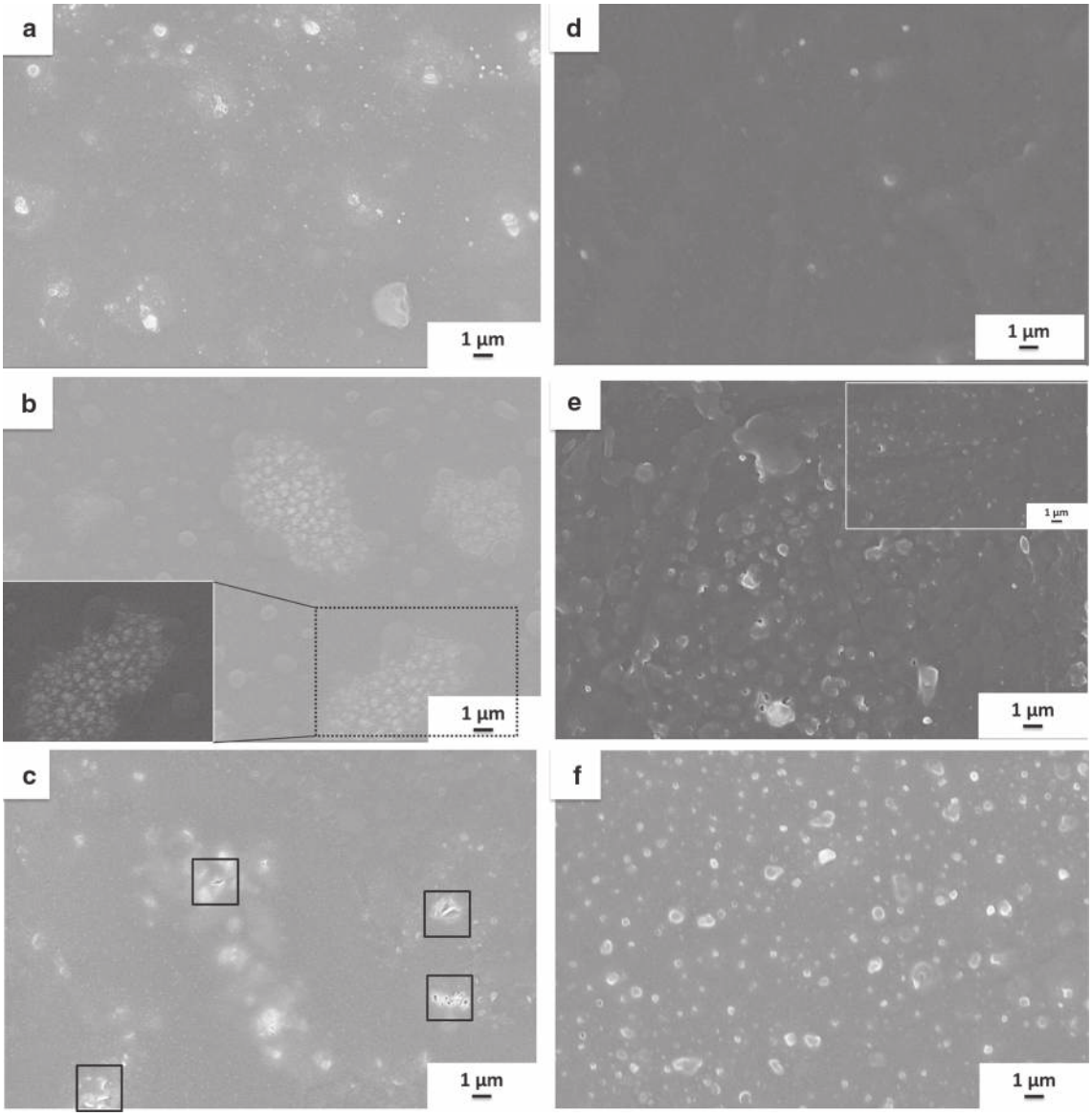

Figure 3. FESEM images of glass substrates with aluminium oxide seed layer subjected to magnetic stirring for (**a**) 10, (**b**) 20 and (**c**) 30 min; and glass substrates without aluminium oxide seed layer subjected to sonication for (**d**) 10, (**e**) 20 and (**f**) 30 min.

branch-like morphology (figure 2f, g). Based on FESEM analysis of sonicated surfaces, it is clear that the entire substrate is covered with wall-like network nanostructures. The network-like morphology can provide sufficient surface roughness and trap more air in the structure [7], thereby making it suitable for superhydrophobic applications.

Figure 3 delineates the role of sonochemical method and aluminium oxide seed layer independently on the morphology of ZnO nanostructures. Figure 3a–c represents the morphological features of ZnO nanostructures fabricated using technique 2; i.e., without sonication. It is clear that in the absence of sonication process, the formation of nanoparticles was sparse and agglomeration of nanoparticles was increasing with increase in deposition time. The agglomerated particles were clearly visible in the high-magnification image of the inset of figure 3b. Evolution of a small fraction of nanowalls from the aluminium oxide seed layer could be observed after 30 min of magnetic stirring and it is represented in figure 3c. It has to be noted that the ZnO nanowall formation was initiated after 30 min in the magnetic stirring (technique 2), while the same was initiated immediately within 5 min of sonication process (technique 1).

Figure 3d–f depicts the morphological features of ZnO nanostructures at various processing times using technique 3; i.e., sonication process without aluminium oxide seed layer. It is observed from figure 3d that during 10 min of

sonication, ZnO nanoparticles were sparsely deposited on the glass substrates. While in figure 3e and f, a large number of ZnO nanoparticles were uniformly deposited over the glass substrates. It is clear that the density of ZnO nanoparticles deposited on the glass substrates increased as a function of sonication time, thereby reduced the gaps between the deposited nanoparticles. It can also be seen that the morphology of the ZnO nanoparticles sonochemically deposited without aluminium oxide seed layer (figure 3) differs from the morphology of ZnO nanowalls deposited with aluminium oxide seed layers (figure 2). On the basis of morphological analysis, it can be concluded that the presence of aluminium oxide seed layer is the solitary reason for the formation of ZnO nanowall structure. The rate of formation of nanowalls remains faster in the sonication technique when compared to magnetic stirring, although aluminium oxide seed layer is available in both the cases.

Based on the morphological evolution observed in the ultrasonic-assisted deposition of ZnO nanostructures over aluminium oxide-seeded substrates (from figure 2b–g), a possible growth mechanism for the formation of ZnO nanowalls is proposed and it is schematically illustrated in figure 4. The aluminium oxide seed layer deposited over the glass substrates acts as heterogeneous nucleation sites for the growth of ZnO nanowalls (figure 4a) [7]. When aluminium oxide layer-seeded glass substrates is introduced in the equimolar precursor solution of $Zn(NO_3)_2 \cdot 6H_2O$ and $(CH_2)_6N_4$, Al in the seed layer undergoes chemical reaction leading to the formation of $Al(OH)^{4-}$ in the alkaline condition. $Al(OH)^{4-}$ ions thus formed on the surface of seeded substrate binds to Zn^{2+} ions in the solution, which blocks the growth of ZnO in [001] direction; thereby enhancing the growth of ZnO in lateral directions (figure 4b) [9]. Upon sonication, high vapour pressure created in the solution leads to faster dissociation of $Zn(NO_3)_2 \cdot 6H_2O$ and $(CH_2)_6N_4$ compounds and formation of Zn^{2+} and OH^- ions in the precursor solution [10]. Hence, there occurs a rapid growth of ZnO planes (0−10), (−110), (101) and (−100) in the lateral direction (figure 4c) [10–13]. As the sonication process proceeds further, lateral growth of ZnO nanowalls occur and cease their growth when they collide with other neighbouring nanowalls. Finally, the individual ZnO nanowalls can get interlinked with each other; thereby forming dense nanowall-like network structures (figure 4d). Thus, aluminium oxide seed layer and sonochemical process have synergistically aided in the formation of dense ZnO nanowalls in short duration.

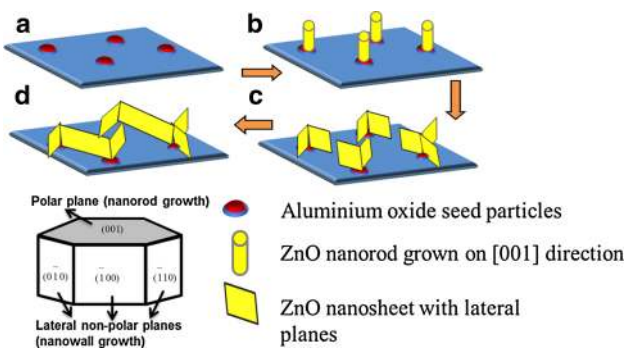

Figure 4. Schematic representation for the formation of ZnO nanowalls in the presence of aluminium oxide seed layer and sonication technique.

Figure 5 shows the comparison of the AFM topographical image of ZnO nanostructures fabricated over glass substrates after 20 min of processing using different techniques. In sample S1 (fabricated using technique 1), a dense layer of randomly oriented nanostructures was observed (figure 5a). On the other hand, in sample S2 (fabricated using technique 2), a very small amount of nanoparticles was identified (figure 5b). It suggested that the kinetics of nanostructures formation is slow in the case of magnetic stirring, i.e., in the absence of sonication [2]. In the case of sample S3 (fabricated using technique 3), uniform distribution of sparse nanoparticles is detected over the substrate (figure 5c). These observations correlate well with the corresponding FESEM images in figures 2 and 3. In the case of technique 3, the ZnO nanoparticles were formed according to the following reactions (1–4):

$$(CH_2)_6N_4 + 10H_2O \xrightarrow{\gg} 6HCHO + 4NH_4^+ + 4OH^- \quad (1)$$

$$Zn(NO_3)_3 \cdot 6H_2O \xrightarrow{\gg} Zn^{2+} + 3NO_3^- + 6H_2O \quad (2)$$

$$Zn^{2+} + 4OH^- \xrightarrow{\gg} Zn(OH)_4^{2-} \quad (3)$$

$$Zn(OH)_4^{2-} \xrightarrow{\gg} ZnO + 2OH^- + H_2O \quad (4)$$

In this process, generation of ZnO nanoparticles occurs in the solution phase and it is subsequently deposited on the glass substrate during sonication. The suspended ZnO nanoparticle reaches the glass surface at very high velocity during sonication process. This technique can cause local heating of the glass substrate when nanoparticles impinge on the surface [14] and such observation is clearly visible in figure 5c.

The fabricated surfaces were compared in terms of statistical parameters extracted from the AFM images and it is presented in table 1. Several statistical parameters such as average roughness, RMS roughness and surface skewness are used to quantify the morphological changes. The average roughness and RMS roughness are the most commonly used descriptor of surface roughness. Surface skewness is a measure of symmetry of the statistical distribution of valleys and peaks in the sample. Skewness value equal to 0 implies that the surface has evenly distributed peaks and valleys of specific heights. Surface profiles with more valleys than peaks indicate negative skewness, whereas a surface with peaks larger than valleys represents positive skewness [15]. In the present work, the surface roughness (average as well as RMS)

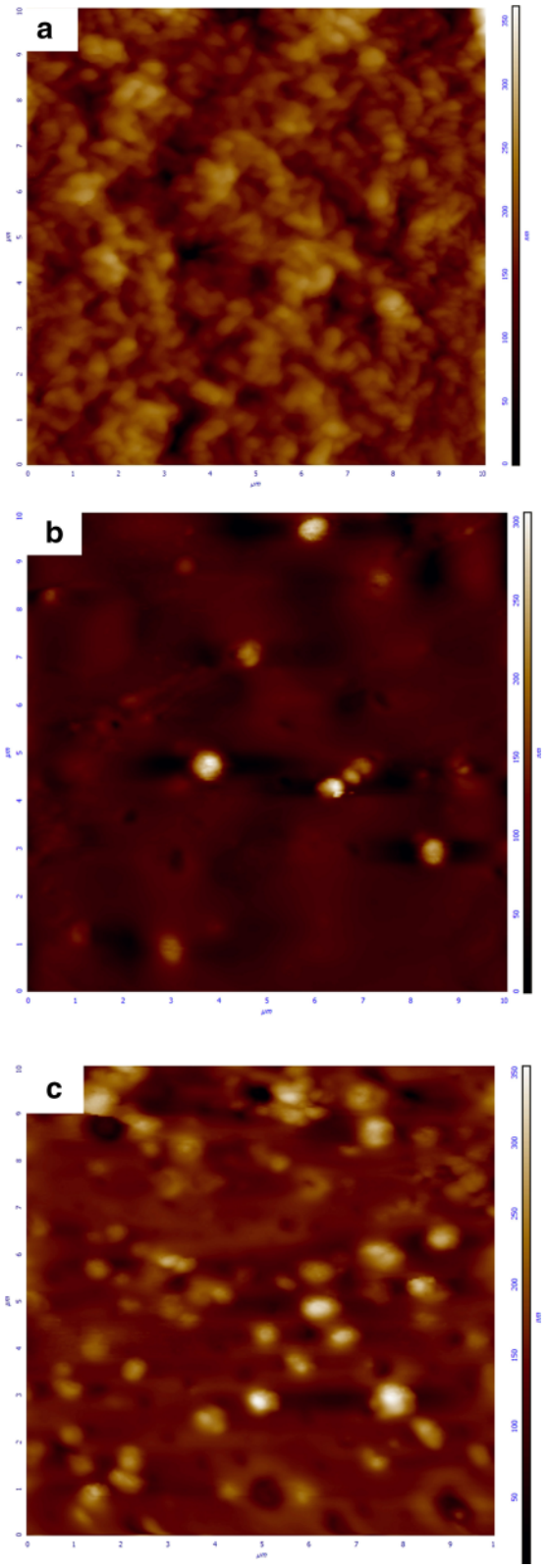

Figure 5. AFM images of ZnO nanostructures fabricated over glass substrates after 20 min processing using (**a**) technique 1 (sample S1), (**b**) technique 2 (sample S2) and (**c**) technique 3 (sample S3).

is found to be highest for sample S1, then it is followed by sample S3 and subsequently sample S2. This implies that sonication technique provides high surface roughness to the samples (samples S1 and S3) when compared with samples obtained without sonication process (sample S2). From table 1, it is clear that the surface skewness value for sample S1 is negative, while it is positive for samples S2 and S3. Hence, it can be inferred that the surface of the sample S1 covered with more valleys (or pores) compared to peaks favourable for superhydrophobic property.

Surface morphology and the distribution of nanostructures over the surface can have a profound effect on the wettability of surfaces. Wettability studies usually involve the measurement of contact angles as a primary option to indicate the degree of solid/liquid interface interactions. The static water contact angle of fabricated ZnO nanostructures with respect to reaction time is shown in figure 6. According to figures 2 and 3, the surface morphology of zinc oxide nanostructures are significantly changed by the sonication time and fabrication techniques adopted in the present work. Correspondingly, the wettability of such surfaces is found to be distinctly varied with respect to those parameters. All the fabricated surfaces after chemical modification has shown hydrophobic behaviour with static water contact angle greater than 90°. In the case of sonicated samples, the static contact angle values showed increasing trend from 105° with increase in sonication time and the highest value of contact angle was obtained as 156° after 20 min of sonication time (figure 6a). Further increase in sonication time to 30 min results in decrease of contact angle to 150°. The contact angle values can be directly related to the density of nanostructures and the presence of air pockets within such structures [16]. The air entrapped within the nanostructures balances the weight of the water droplet and low surface energy of the substrate permits the fabricated surface to have superhydrophobic property. The aforementioned mechanism can be attributed to the superhydrophobic nature of 20-min sonicated samples. With further increase of sonication time, the density of nanowalls continues to increase and can fill up the air gap between the nanowalls leading to the decrease in the contact angle values [17]. This could be the possible reason for the observation of decrease in contact angle of 30-min sonicated samples.

The static contact angle values of ZnO nanostructures fabricated using techniques 2 (figure 6b) and 3 (figure 6c) have shown maximum static contact angle of 120°. The reason for obtaining hydrophobic nature instead of superhydrophobic property might be suggested due to the lack of favourable dense nanostructures to hold air pockets within. The observation of low contact angle value of surface fabricated using techniques 2 and 3 also can be correlated with the statistical parameters such as reduced surface roughness and positive values of surface skewness compared to technique 1. In a nutshell, the presence of aluminium oxide seed layer and sonochemical condition synergistically contribute to the density and morphology of the ZnO nanowalls structure and

Table 1. Statistical parameters of surfaces fabricated for 20 min by techniques 1, 2 and 3.

Substrates	Untreated glass substrate	Sample S1	Sample S2	Sample S3
Average roughness (nm)	1.5558	34	21	15
RMS roughness (nm)	1.8467	43	31	23
Surface skewness	0.0307	−0.197	0.94	2.32
Static contact angle (°)	—	156	118	105

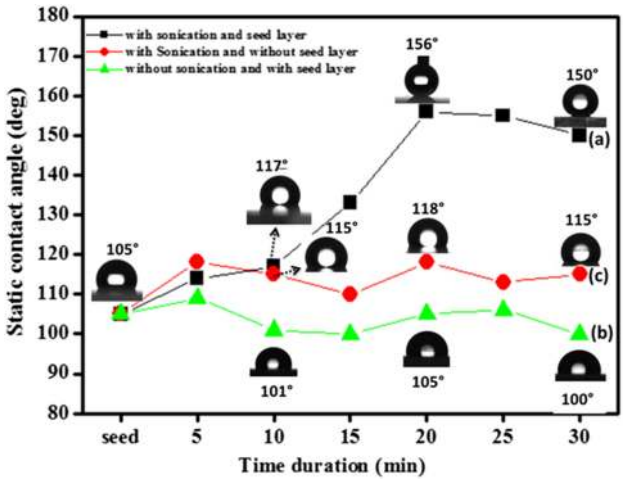

Figure 6. Static contact angle values of ZnO nanostructures with respect to time duration: (**a**) technique 1, (**b**) technique 2 and (**c**) technique 3.

correspondingly the superhydrophobic properties of the fabricated surface.

Conclusions

In summary, well-defined ZnO nanowalls were successfully fabricated on aluminium oxide-seeded glass substrates using the sonochemical deposition method. The sonochemically fabricated samples were exhibiting superhydrophobicity with static water contact angle of 156°. The experimental analysis suggested that the aluminium oxide seed layer deposition is the solitary reason for the formation of nanowalls. When compared to simple magnetic stirring, the adoption of sonochemical technique increases the rate of ZnO formation to many folds. The synergistic effect of the aluminium oxide seed layer and sonochemical process aided in the dense growth of ZnO nanowalls network in short duration, which in turn paves the way to achieve superhydrophobic property. The present study illustrates that the sonochemical method is a relatively simple, kinetically faster and potentially scalable strategy to produce ZnO nanostructures with superhydrophobic property on glass substrates.

Acknowledgement

This work was financially supported by DST–SERB, Government of India, under JC Bose National Fellowship (File. No. SR/S2/JCB-58/2011, 28.11.2011).

References

[1] Yu S, Guo Z and Liu W 2015 *ChemCommun.* **51** 1775
[2] Jung S-H, Oh E, Lee K-H, Park W and Jeong S-H 2007 *Adv. Mater.* **19** 749
[3] Perelshtein I, Applerot G, Perkas N, Wehrschetz-Sigl E, Hasmann A and Guebitz G M 2009 *Appl. Mater. Interfaces* **1** 361
[4] Oh E, Choi H-Y, Jung S-H, Cho S, Kim J C, Lee K-H *et al* 2009 *Sens. Actuators B* **141** 239
[5] Nayak A P, Katzenmeyer A M, Kim J-Y, Kwon M K, Gosho Y and Islam M S 2010 *Proc. SPIE* **7683** 768312
[6] Okyay T O, Bala R K, Nguyen H N, Atalay R, Bayam Y and Rodrigues D F 2015 *RSC Adv.* **5** 2568
[7] Wang T, Liu Y, Li G, Sun Z, Lu J, Liu B *et al* 2011 *CrystEngComm.* **13** 2661
[8] Yu J, Li Q, Hao Y F, Kuang S Y, Bai X D, Chong Y M *et al* 2010 *ACS Nano* **4** 414
[9] Tang J-F, Su H-H, Lu Y-M and Chu S-Y 2015 *CrystEngComm.* **17** 592
[10] Suslick K S, Gawienowski J J, Schubert P F and Wang H H 1984 *Ultrasonics* **22** 33
[11] Lee G-H 2010 *Ceram. Int.* **36** 1871
[12] Yu H, Zhang Z, Han M, Hao X and Zhu F 2005 *J. Am. Chem. Soc.* **127** 2378
[13] Mason T J 1986 *Ultrasonics* **24** 245
[14] Yuan Y and Lee T R 2013 *Surface science techniques* Bracco G and Holst B (ed) (Berlin Heidelberg: Springer) p 3
[15] Peltonen J, Jarn M, Areva S, Linden M and Rosenholm J B 2004 *Langmuir* **20** 9428
[16] Gurav A B, Latthe S S and Vhatkar R S 2013 *Surf. Innov.* **1** 176
[17] Guo Z, Chen X, Li J, Liu J H and Huang X J 2011 *Langmuir* **27** 6193